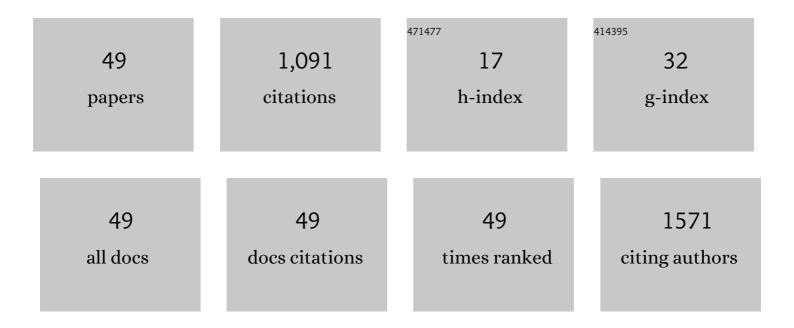
## Hajime Hojo

List of Publications by Year in descending order

Source: https://exaly.com/author-pdf/826740/publications.pdf Version: 2024-02-01



HALIME HOLO

#	Article	IF	CITATIONS
1	Atomic Structure of a CeO <sub>2</sub> Grain Boundary: The Role of Oxygen Vacancies. Nano Letters, 2010, 10, 4668-4672.	9.1	173
2	Enhanced Piezoelectric Response due to Polarization Rotation in Cobaltâ€Substituted BiFeO <sub>3</sub> Epitaxial Thin Films. Advanced Materials, 2016, 28, 8639-8644.	21.0	72
3	Development of Bismuth Ferrite as a Piezoelectric and Multiferroic Material by Cobalt Substitution. Advanced Materials, 2018, 30, e1705665.	21.0	66
4	A-Site and B-Site Charge Orderings in an <i>s–d</i> Level Controlled Perovskite Oxide PbCoO <sub>3</sub> . Journal of the American Chemical Society, 2017, 139, 4574-4581.	13.7	52
5	Realization of Large Electric Polarization and Strong Magnetoelectric Coupling in BiMn <sub>3</sub> Cr <sub>4</sub> O <sub>12</sub> . Advanced Materials, 2017, 29, 1703435.	21.0	50
6	Melting of Pb Charge Glass and Simultaneous Pb–Cr Charge Transfer in PbCrO <sub>3</sub> as the Origin of Volume Collapse. Journal of the American Chemical Society, 2015, 137, 12719-12728.	13.7	45
7	Ferromagnetism at Room Temperature Induced by Spin Structure Change in BiFe <sub>1â^²</sub> <i><sub>x</sub></i> Co <i><sub>x</sub></i> O <sub>3</sub> Thin Films. Advanced Materials, 2017, 29, 1603131.	21.0	45
8	Photocatalytic oxidation process for treatment of gas phase benzene using Ti3+ self-doped TiO2 microsphere with sea urchin-like structure. Chemical Engineering Journal, 2020, 402, 126220.	12.7	41
9	Temperature-Independent, Large Dielectric Constant Induced by Vacancy and Partial Anion Order in the Oxyfluoride Pyrochlore Pb <sub>2</sub> Ti <sub>2</sub> O <sub>6â^îſ</sub> F <sub>2ſ</sub> . Chemistry of Materials, 2016, 28, 5554-5559.	6.7	38
10	Efficient visible light photocatalysis enabled by the interaction between dual cooperative defect sites. Applied Catalysis B: Environmental, 2020, 274, 119099.	20.2	34
11	Atomic structure and strain field of threading dislocations in CeO2 thin films on yttria-stabilized ZrO2. Applied Physics Letters, 2011, 98, 153104.	3.3	32
12	Room-temperature ferrimagnetic semiconductor 0.6FeTiO3â^™0.4Fe2O3 solid solution thin films. Applied Physics Letters, 2006, 89, 142503.	3.3	30
13	New PbTiO <sub>3</sub> -Type Giant Tetragonal Compound Bi <sub>2</sub> ZnVO <sub>6</sub> and Its Stability under Pressure. Chemistry of Materials, 2015, 27, 2012-2017.	6.7	30
14	Enhanced Negative Thermal Expansion Induced by Simultaneous Charge Transfer and Polar–Nonpolar Transitions. Journal of the American Chemical Society, 2019, 141, 19397-19403.	13.7	30
15	Large Negative Thermal Expansion Induced by Synergistic Effects of Ferroelectrostriction and Spin Crossover in PbTiO <sub>3</sub> -Based Perovskites. Chemistry of Materials, 2019, 31, 1296-1303.	6.7	29
16	Direct Observation of Magnetization Reversal by Electric Field at Room Temperature in Co-Substituted Bismuth Ferrite Thin Film. Nano Letters, 2019, 19, 1767-1773.	9.1	23
17	Controlling Diphenyl Ether Hydrogenolysis Selectivity by Tuning the Pt Support and H-Donors under Mild Conditions. ACS Catalysis, 2021, 11, 12661-12672.	11.2	20
18	Removal of benzene by non-thermal plasma catalysis over manganese oxides through a facile synthesis method. Environmental Science and Pollution Research, 2019, 26, 8237-8247.	5.3	19

Најіме Нојо

#	Article	IF	CITATIONS
19	Structural evolution and enhanced piezoresponse in cobalt-substituted BiFeO <sub>3</sub> thin films. Applied Physics Express, 2014, 7, 091501.	2.4	18
20	A new LiNbO3-type polar oxide with closed-shell cations: ZnPbO3. Journal of Applied Physics, 2015, 118, .	2.5	17
21	Effect of catalyst composition and reactor configuration on benzene oxidation with a nonthermal plasma-catalyst combined reactor. Catalysis Today, 2019, 332, 144-152.	4.4	17
22	Observation of novel charge ordering and spin reorientation in perovskite oxide PbFeO3. Nature Communications, 2021, 12, 1917.	12.8	17
23	Enhanced catalytic performance of spinel-type Cu-Mn oxides for benzene oxidation under microwave irradiation. Journal of Hazardous Materials, 2022, 424, 127523.	12.4	16
24	Atomic and Electronic Structure of Pt/TiO <sub>2</sub> Catalysts and Their Relationship to Catalytic Activity. Nano Letters, 2022, 22, 145-150.	9.1	16
25	High-Temperature Monoclinic <i>Cc</i> Phase with Reduced <i>c</i> / <i>a</i> Ratio in Bi-based Perovskite Compound Bi <sub>2</sub> ZnTi <sub>1–<i>x</i></sub> Mn <sub><i>x</i></sub> O <sub>6</sub> . Inorganic Chemistry, 2016, 55, 6124-6129.	4.0	12
26	Systematic charge distribution changes in Bi- and Pb-3d transition metal perovskites. Dalton Transactions, 2018, 47, 1371-1377.	3.3	12
27	Catalytic Removal of Benzene at Mild Temperature over Manganese Oxide Catalysts. Catalysis Surveys From Asia, 2019, 23, 199-209.	2.6	12
28	Perovskite-Type CuNbO <sub>3</sub> Exhibiting Unusual Noncollinear Ferrielectric to Collinear Ferroelectric Dipole Order Transition. Chemistry of Materials, 2020, 32, 5016-5027.	6.7	11
29	Polarization Rotation at Morphotropic Phase Boundary in New Lead-Free Na <sub>1/2</sub> Bi <sub>1/2</sub> V <sub>1–<i>x</i></sub> Ti <i><sub><i>x</i></sub></i> O <sub>3</sub> Piezoceramics. ACS Applied Materials & Interfaces, 2021, 13, 5208-5215.	8.0	11
30	Functional Transition Metal Perovskite Oxides with 6 <i>s</i> <sup>2</sup> Lone Pair Activity Stabilized by High-Pressure Synthesis. Annual Review of Materials Research, 2021, 51, 329-349.	9.3	11
31	Fabrication of p-type ferrimagnetic semiconductor thin films based on FeTiO3–Fe2O3 solid solution. Journal of Magnetism and Magnetic Materials, 2007, 310, 2105-2107.	2.3	10
32	Room temperature ferromagnetism in BiFe1â^' <i>x</i> Mn <i>x</i> O3 thin film induced by spin-structure manipulation. Applied Physics Letters, 2018, 112, .	3.3	10
33	Analysis of TEM images of metallic nanoparticles using convolutional neural networks and transfer learning. Journal of Magnetism and Magnetic Materials, 2021, 538, 168225.	2.3	9
34	Sodium titanium oxide bronze nanoparticles synthesized <i>via</i> concurrent reduction and Na <sup>+</sup> -doping into TiO <sub>2</sub> (B). Nanoscale, 2019, 11, 1442-1450.	5.6	8
35	Catalyst design of Pt/TiO2 microsphere for benzene oxidation under microwave irradiation. Catalysis Today, 2021, 376, 285-291.	4.4	8
36	Rational Design of Cu-Doped ZnS Nanospheres for Photocatalytic Evolution of H <sub>2</sub> with Visible Light. ACS Applied Energy Materials, 2022, 5, 1849-1857.	5.1	8

Најіме Нојо

#	Article	IF	CITATIONS
37	Insights into the Hydrogenolysis Mechanism of Diphenyl Ether over Cl-Modified Pt/γ-Al <sub>2</sub> O <sub>3</sub> Catalysts by Experimental and Theoretical Studies. ACS Sustainable Chemistry and Engineering, 2022, 10, 8897-8907.	6.7	7
38	High-Pressure Synthesis of the Cobalt Pyrochlore Oxide Pb <sub>2</sub> Co <sub>2</sub> O <sub>7</sub> with Large Cation Mixed Occupancy. Inorganic Chemistry, 2017, 56, 11676-11680.	4.0	6
39	Magnetic properties of disordered ferrite and ilmenite–hematite thin films. Journal of Magnetism and Magnetic Materials, 2009, 321, 818-821.	2.3	4
40	Modulating the Structure and Magnetic Properties of ε-Fe <sub>2</sub> O <sub>3</sub> Nanoparticles via Electrochemical Li <sup>+</sup> Insertion. Inorganic Chemistry, 2020, 59, 4357-4365.	4.0	4
41	Topochemical synthesis of perovskite-type CuNb <sub>2</sub> O <sub>6</sub> with colossal dielectric constant. Journal of Materials Chemistry C, 2021, 9, 13981-13990.	5.5	4
42	Photocatalytic hydroxylation of benzene to phenol with dioxygen using sodium decatungstate. Molecular Catalysis, 2021, 515, 111933.	2.0	4
43	Piezoelectric Materials: Enhanced Piezoelectric Response due to Polarization Rotation in Cobalt-Substituted BiFeO3 Epitaxial Thin Films (Adv. Mater. 39/2016). Advanced Materials, 2016, 28, 8785-8785.	21.0	3
44	Magnetic Ordering and Structural Transition in the Ordered Double-Perovskite Pb <sub>2</sub> NiMoO <sub>6</sub> . Chemistry of Materials, 2022, 34, 97-106.	6.7	3
45	Band Engineering-Tuned Localized Surface Plasmon Resonance in Diverse-Phased Cu <sub>2–<i>x</i></sub> S <sub><i>y</i></sub> Se <sub>1–<i>y</i></sub> Nanocrystals. Journal of Physical Chemistry C, 2022, 126, 8107-8112.	3.1	3
46	Mapping electrostatic potential around a Pt nanoparticle supported on TiO2 (110). Microscopy and Microanalysis, 2021, 27, 2308-2309.	0.4	1
47	Automatic Hologram Acquisition of Pt Catalyst Nanoparticles on TiO2 Using Particle Detection with Image Processing and Al Classification. Microscopy and Microanalysis, 2021, 27, 252-253.	0.4	0
48	Fabrication and characterization of La-added MgFe2O4 as catalyst support for CO oxidation. Ceramics International, 2021, 47, 32786-32786.	4.8	0
49	Enhanced Piezoelectric Response in Orientation-Controlled BiFe1–xGaxO3 Thin Films with Polarization Rotation. ACS Applied Electronic Materials, 0, , .	4.3	0